Stabilizing viscosity contrast effect on miscible displacement in heterogeneous porous media, using lattice Bhatnagar–Gross–Krook simulations

Laurent Talon,[a] Jérôme Martin,[b] Nicole Rakotomalala,[c] and Dominique Salin[d]

Laboratoire FAST, Bâtiment 502, Campus Universitaire, 91405 Orsay Cedex, France

We analyze the displacement of a viscous fluid by a miscible more viscous one in heterogeneous porous media. We performed lattice Bhatnagar–Gross–Krook simulations, which were previously successfully applied to the study of the dispersion of a passive tracer in a stochastic heterogeneous porous medium. In the present situation, the flow is stable (no viscous fingering) and leads to an overall Gaussian dispersion, the coefficient of which decreases as the viscosity ratio increases. The results are in reasonable agreement with the stochastic approach of Welty and Gelhar. © *2004 American Institute of Physics.* [DOI: 10.1063/1.1810474]

I. INTRODUCTION

One key issue in hydrology, contaminant remediation, and petroleum engineering is the understanding of the coupling between the porous medium heterogeneity and the fluid displacement properties given by buoyancy or viscosity effects. In this paper, we will focus on the viscous effect related to the displacement of a less viscous fluid in the porous medium by a more viscous fluid: This displacement is stable, as opposed to the well-known situation where a more viscous fluid is displaced by a less viscous one. If the latter case of viscous fingering has been extensively studied in homogeneous porous media (of permeability uniform in space),[1–3] it is not the case for realistic, i.e., heterogeneous porous media. A number of investigations[4–11] have addressed the issue of the coupling between a destabilizing viscosity contrast and the permeability distribution. Basically, in a heterogeneous porous medium, the fluid flows through the hydrodynamically easiest path that is through the larger permeability path, leading to an enhanced effect of heterogeneities, such as "resonance" between the intrinsic scale of the fingers (in homogeneous medium) and the correlation length of the heterogeneous porous medium.[5,6,9]

Curiously enough, little attention has been paid to the case of stabilizing viscous effects in displacements in heterogeneous porous media. Let us mention an experiment in a layered porous medium,[8] where the resulting stratification of the displacement parallel to the layers was reduced and even suppressed for a large enough stabilizing viscosity ratio.

In the present paper, using our lattice BGK (Bhatnagar–Gross–Krook) simulation method,[12] well suited for tracer macrodispersion in heterogeneous porous media,[13–15] we address the issue of miscible stable displacements in more realistic heterogeneous porous media, namely, those with given log-normal permeability distributions and correlation lengths. We find that the mixing front between the fluids exhibits Gaussian dispersion, the dispersion coefficient of which decreases when the viscosity ratio increases. The results are shown to compare reasonably well with the extrapolation of the predictions by Welty and Gelhar[16] to our case.

II. NUMERICAL SIMULATIONS

As detailed in Ref. 12, the permeability field $K(\vec{r})$ of the porous medium was chosen to obey a log-normal distribution

$$\ln[K(\vec{r})] = \bar{f} + f'(\vec{r}), \tag{1}$$

where $\bar{f}$ is the mean of the distribution and where the perturbation field $f'(\vec{r})$ has a zero mean value and a variance σ_f^2. The isotropic spatial correlation of the permeability field is given by the exponential decay of the covariance function of f',

$$R_{ff}(\vec{\zeta}) = E[f'(\vec{r})f'(\vec{r} + \vec{\zeta})] = \sigma_f^2 \exp\left(-\frac{\zeta}{\lambda}\right) \tag{2}$$

with λ the correlation length. Such a porous medium was generated by convolving a random white noise field with an *ad hoc* correlation function, namely,

$$h(x,y) = \exp[(x^2/\delta^2 + y^2/\delta^2)^{1/3}], \tag{3}$$

where the value of the parameter δ sets that of the correlation length λ. Note that the characteristic value of the resulting permeability field is $K_l = \exp(\bar{f})$.

We then study the displacement in the porous medium of a fluid of viscosity μ_1 by another fluid of viscosity μ_2, miscible to the first one, and flowing at the constant mean rate q_0 in the x direction. To achieve this, we perform the simulation of the following equations for the velocity field $\vec{q}$ and the concentration C of the injected fluid:

$$\vec{\nabla} \cdot \vec{q} = 0, \tag{4}$$

$$\vec{\nabla} P = -\frac{\mu}{K(\vec{r})}\vec{q} + \mu\Delta\vec{q}, \tag{5}$$

[a] Electronic mail: laurent.talon@normalesup.org
[b] Electronic mail: martin@fast.u-psud.fr
[c] Electronic mail: rako@fast.u-psud.fr
[d] Electronic mail: dos@fast.u-psud.fr

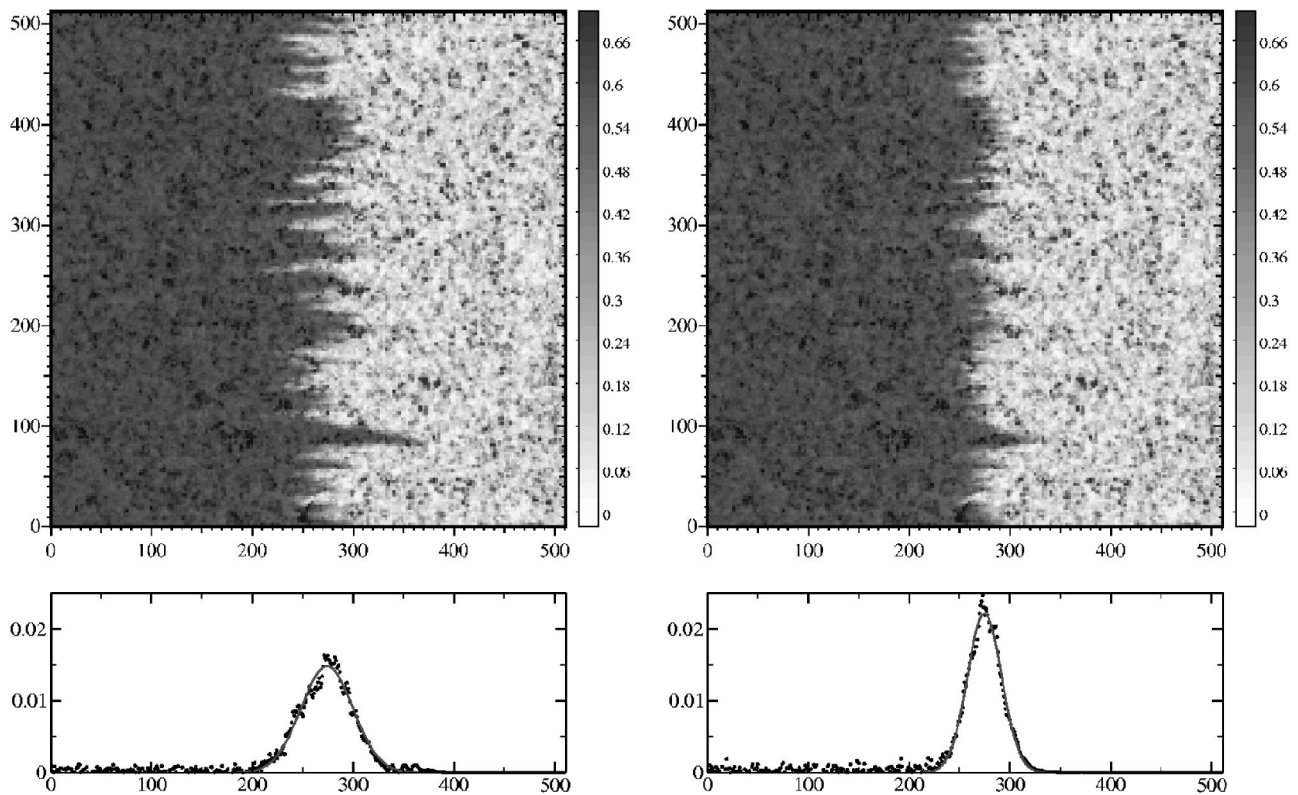   4408   © 2004 American Institute of Physics

FIG. 1. The top figures show typical injected fluid patterns (in dark gray) for the tracer case, $\mu_2/\mu_1=1$ ($\beta=0$, left) and for $\mu_2/\mu_1=1.22$ ($\beta=0.2$, right). The permeability field (given by the gray-level background) and the flow parameters are the same: $\lambda=2$, $\sigma_f=0.8$, $q_0=4\times10^{-3}$, $D_m=5\times10^{-5}$. The bottom figures display the measured absolute value of the mean concentration gradient, $-(\partial\bar{C}/\partial x)$ (dots), and the data fit to a Gaussian behavior (lines), as functions of the distance x to the injection plane.

$$\frac{\partial C}{\partial t} + \vec{q}\cdot\vec{\nabla}C = D_m\Delta C. \tag{6}$$

We note that the flow equation [Eq. (5)] involves a Brinkman-like term, $\mu\Delta\vec{q}$, the influence of which on tracer macrodispersion was analyzed in a previous paper.[12] Following Refs. 16 and 17, the fluid viscosity μ is assumed to have an exponential concentration dependence, namely,

$$\mu(C) = \mu_1\exp(\beta C), \tag{7}$$

where

$$\beta = \ln\left(\frac{\mu_2}{\mu_1}\right). \tag{8}$$

The case $\beta>0$ corresponds to a stable displacement, whereas $\beta<0$ corresponds to an unstable one (viscous fingering). Note also that the concentration C undergoes an isotropic mesoscopic diffusion of coefficient D_m [Eq. (6)], leading to the same value of the mesoscopic longitudinal and transverse dispersivities: $\alpha_L=\alpha_T=D_m/q_0$.

The simulations presented here were performed on typical mesh sizes 512×512 and during 150 000 time steps, using a 1.7 GHz Pentium IV. They were characterized by a Brinkman parameter $K_l/\lambda^2\ll1$, which mimimizes the effect of the Brinkman term, and a variance σ_f^2 of the permeability

distribution ranging in [0, 1]. Typical mean flow rate q_0, viscosity ratio μ_2/μ_1 (and thus β), and diffusion coefficient D_m ranged in [0.001, 0.01], [1, 2.5] ($\beta\in[0,0.9]$) and [$5\times10^{-5},10^{-3}$], respectively. In such conditions, the CPU time was about 10 h.

Figure 1 (top) shows typical invasion patterns, on the same permeability distribution, for tracer dispersion ($\mu_2/\mu_1=1$, $\beta=0$, left) and for a stable displacement ($\mu_2/\mu_1=1.22$, $\beta=0.2$, right). Even for this viscosity ratio close to 1, the sharpening of the mixing front is clearly observed, compared to the tracer case. An estimate of the front width is obtained by computing the derivative of the mean concentration profile $\bar{C}(x)$ (dots in Fig. 1, bottom). Then the so-obtained mean concentration gradients are fitted tentatively to Gaussian profiles (solid lines in Fig. 1, bottom). Note that such a Gaussian behavior is reached at long times, for a spreading of the mixing front in the mean flow direction large enough compared to the correlation length of the permeability field: Typically a ratio of those quantities of the order of 20 was necessary to obtain Gaussian profiles.

From these profiles, one measures the variance $\sigma^2(t)$ at time t. The time evolution of σ^2 for the invasion pattern of Fig. 1, right, is displayed in Fig. 2. One notices that σ^2 indeed varies nearly linearly with time at long times. Therefore an effective diffusion coefficient D_{eff} can be measured using the relation,
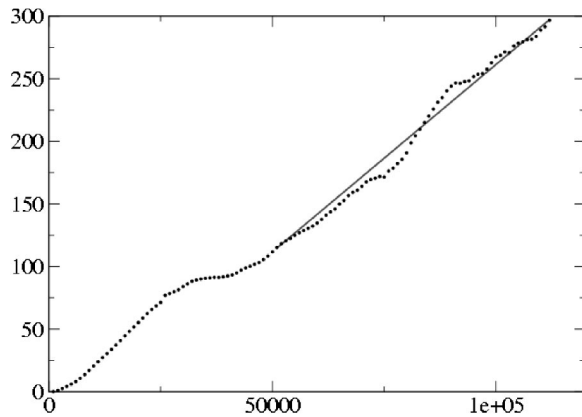
FIG. 2. Half of variance of the mean concentration gradient, $\frac{1}{2}\sigma^2$ (dots), vs time for the simulation of Fig. 1, right. The line is a linear regression fit of the data. Here, we obtain $D_{eff}=5\times10^{-3}$.

FIG. 3. Normalized effective diffusion coefficient, $D_{eff}/q_0\lambda\sigma_f^2$, vs the parameter $b_M=-(\beta\lambda^2/\alpha_T)(\partial\bar{C}/\partial x)|_{Max}$, for different values of the control parameters q_0, β, D_m, and σ_f^2 (symbols). Each symbol corresponds to the variation of one parameter at a time. The lines give the prediction of Eq. (10), using the values $b=b_M$ (solid line), $b=b_M/2$ (dashed), and $b=b_M/3$ (dot-dashed).

$$\frac{1}{2}\frac{d\sigma^2}{dt}=D_{eff}.$$

This diffusive behavior was observed whatever the values of q_0, β, D_m, and σ_f used (in the ranges given above): This supports the contention that the mixing regime is diffusive in our range of parameters.

III. THEORY

Before proceeding to the data analysis, let us summarize the analytical derivation of the macroscopic dispersion coefficient in a viscously stabilizing two-dimensional displacement in a heterogeneous porous medium. For this purpose, we follow the same approach as in Refs. 16 and 12 and use the permeability field [Eqs. (1) and (2)] and the flow equations [Eqs. (4), (5), (7), and (8)] detailed above. The diffusion equation of the concentration C is written in the form

$$\frac{\partial C}{\partial t}+\vec{q}\cdot\vec{\nabla}C=\frac{\partial}{\partial x}\left(q_0\alpha_L\frac{\partial C}{\partial x}\right)+\frac{\partial}{\partial y}\left(q_0\alpha_T\frac{\partial C}{\partial y}\right) \qquad (9)$$

in order to investigate the roles of α_L and α_T, respectively. We assume small perturbations about the transversely averaged values for the concentration, the velocity, and the pressure: $C=\bar{C}(x)+C'$, $\vec{q}=q_0\vec{u}_x+\vec{q}'$, $P=P(x)+P'$. Viscosity and permeability fields become, respectively,

$$\mu(C)=\mu(\bar{C})+C'\frac{d\mu}{dC}(\bar{C})=\mu(\bar{C})(1+\beta C')$$

and

$$K(\vec{r})=K_l(1+f').$$

The calculation of the mean dispersive flux $\overline{q'C'}$ along the same line as in Ref. 12 then leads to an effective macrodispersivity α, when a uniform mean concentration gradient, $-(\partial\bar{C}/\partial x)$, as in Ref. 16 is assumed. We find after some calculations that the longitudinal macrodispersivity $\alpha=D_{eff}/q_0$, with D_{eff} the effective diffusion coefficient, is given by
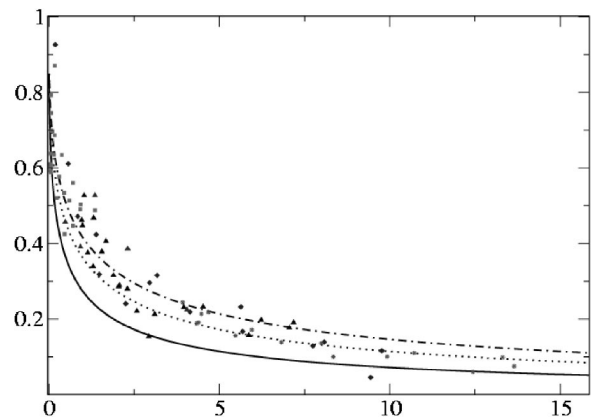
$$\alpha=\lambda\sigma_f^2\int_0^\infty\frac{u^2du}{(1+u^2)^{3/2}\left(1+\dfrac{K_l}{\lambda^2}u^2\right)\left[u^2\left(1+\dfrac{K_l}{\lambda^2}u^2\right)+b\right]} \qquad (10)$$

with $b=-(\beta\lambda^2/\alpha_T)(\partial\bar{C}/\partial x)$. We note that the modelization is not self-consistent, as the description of the front spreading in terms of a diffusive process leads to the definition of a diffusion coefficient which depends on the concentration gradient. However, the model allows the understanding of the interplay between the different physical quantities in the spreading process. More precisely, the above equation [Eq. (10)] shows that the dispersivity depends on the following two dimensionless variables: the Brinkman term K_l/λ^2, the effect of which was previously studied in the tracer case,[12] and the parameter b, which accounts for viscosity contrasts; for $b=0$ the tracer case[12] is retrieved. Note that a finite value of b requires transverse mixing (α_T) and a uniform concentration gradient as in Taylor dispersion.[18] Note also that Eq. (10) agrees with Welty and Gelhar's equation[16] in the limiting case $K_l/\lambda^2\rightarrow0$.

IV. RESULTS AND DISCUSSION

The viscosity effects can be quantified by measuring the effective diffusion coefficient D_{eff} in terms of b. As mentioned above, the value of b, which is proportional to the concentration gradient, depends on the location where the latter quantity is measured. Here, we arbitrarily chose the largest concentration gradient in the middle of the front (see Fig. 1), and hence the largest parameter b, namely,

$$b_M=-\frac{\beta\lambda^2}{\alpha_T}\left.\frac{\partial\bar{C}}{\partial x}\right|_{Max}. \qquad (11)$$

Note that in so doing, the theoretical dispersion coefficient [Eq. (10)] is underestimated.

Figure 3 shows the effective diffusion coefficient D_{eff} normalized by the value, $q_0\lambda\sigma_f^2$, obtained in the tracer case

($\beta = 0$ and for $K_l/\lambda^2 \to 0$), versus the parameter b_M. Note that each symbol in Fig. 3 corresponds to the variation of one control parameter (q_0, β, D_m, or σ_f^2) at a time, and that each data point is obtained from one given realization of the porous medium, which induces some scatter in the results. However, the data collapse reasonably well on a single curve. This supports the idea that the front experiences a uniform effective mobility gradient. Figure 3 also displays the theoretical prediction of Eq. (10) (solid line), using the same value b_M as in the simulations. Although the trend is the same as for the simulations, the model underestimates the diffusion coefficient, in accordance with the above remark. Therefore, we also plot in Fig. 3 the analytical curves obtained for smaller mean concentration gradients, corresponding to $b = b_M/2$ and $b = b_M/3$. A better agreement is observed when a mean concentration gradient, typically two times as small as the maximum gradient, is used in the prediction of Eq. (10). Note that as diffusion proceeds, the concentration gradient should decrease in time, leading to a decrease of b. Consequently, the diffusion coefficient predicted by the model should increase in time, leading eventually to the dispersivity of the tracer case, $\alpha(b=0)$, as in Ref. 12. However, the characteristic time for such a process is far beyond our simulation means. For instance, in the conditions of the simulation of Fig. 1, right, the variance $\sigma^2(t)$ should reach the value of 10^6 (compared to a few hundreds at the end of the simulation) for the macrodispersivity of the tracer case to be obtained. We may note also that the increase of the diffusion coefficient in time is a direct consequence of the transverse diffusion, which tends to smooth out the viscosity contrast. This can be compared to the well-known Taylor diffusion in a capillary tube, where the transverse dispersion is responsible for the diffusive regime[18] at long times and to miscible displacements between two plates, in which, for small Peclet numbers and a stable viscosity ratio, a diffusion regime was obtained with a diffusion coefficient equal to that of the Taylor regime (tracer case).[19]

V. CONCLUSION

We studied in this paper the macrodispersion in miscible and stable displacements of a less viscous fluid by a more viscous one in heterogeneous porous media, by means of a lattice BGK simulation method. This method was previously applied to the study of the effect of the Brinkman parameter, K_l/λ^2, on the macrodispersion of a passive tracer in a stochastic heterogeneous porous medium. The present work focused on the quantitative estimation of the stabilizing viscous effects on macrodispersion. We showed that, after some transient time, a diffusivelike mixing regime was reached, the effective diffusion coefficient of which depended on the so-called viscous parameter $b = -(\beta\lambda^2/\alpha_T)(d\bar{C}/dx)$, involving the porous medium correlation length λ, the viscosity contrast β, the transverse dispersion α_T, and the mean concentration gradient $-(d\bar{C}/dx)$ of the injected fluid, as derived in Ref. 16. Although the assumption of a uniform mean concentration gradient of the model was not verified, it was shown that the behavior of the diffusion coefficient as a func-

tion of b in the numerical simulations agreed with the model prediction [Eq. (10)], provided that a value of about half the maximum of the observed gradient was taken to evaluate b.

This work will be extended, in stochastic heterogeneous porous media, to the case of viscosity unstable miscible displacements, and to the interplay between the resulting viscous fingering and the effect of the underlying porous medium heterogeneities.

[1] C.-Y. Chen and E. Meiburg, "Miscible porous media displacements in the quarter five-spot configuration. Part 1. The homogeneous case," J. Fluid Mech. **371**, 233 (1998).

[2] G. M. Homsy, "Viscous fingering in porous media," Annu. Rev. Fluid Mech. **19**, 271 (1987).

[3] G. M. Homsy, "The effect of dispersion on fingering in miscible displacements," in *Disorder and Mixing*, edited by E. Guyon, J. P. Nadal, and Y. Pomeau (Kluwer Academic, Dordrecht,1988), Chap. 11, pp. 237–250.

[4] C.-Y. Chen and E. Meiburg, "Miscible porous media displacements in the quarter five-spot configuration. Part 2. Effects of heterogeneities," J. Fluid Mech. **371**, 269 (1998).

[5] A. De Wit and G. M. Homsy, "Viscous fingering in periodical heterogeneous porous media. II: Numerical simulations," J. Chem. Phys. **107**, 9619 (1997).

[6] A. De Wit and G. M. Homsy, "Viscous fingering in periodically heterogeneous porous media. I: Formulation and linear instability," J. Chem. Phys. **107**, 9609 (1997).

[7] V. Kretz, P. Berest, J. P. Hulin, and D. Salin, "An experimental study of the effects of density and viscosity contrasts on macrodispersion in porous media," Water Resour. Res. **39**, 1032 (2002).

[8] D. Loggia, N. Rakotomalala, and D. Salin, "The effect of mobility gradients on viscous instabilities in miscible flows in porous media," Phys. Fluids **11**, 740 (1999).

[9] C. T. Tan and G. M. Homsy, "Viscous fingering with permeability heterogeneity," Phys. Fluids A **4**, 1099 (1992).

[10] H. A. Tchelepi, F. M. Orr, Jr., N. Rakotomalala, D. Salin, and R. Wouméni, "Dispersion, permeability heterogeneity, and viscous fingering: Acoustic experimental observations and particle-tracking simulations," Phys. Fluids A **5**, 1558 (1993).

[11] Z. M. Yang, Y. C. Yortsos, and D. Salin, "Asymptotic regimes in unstable miscible displacements in random porous media," Adv. Water Resour. **25**, 885 (2002).

[12] L. Talon, J. Martin, N. Rakotomalala, D. Salin, and Y. C. Yortsos, "Lattice BGK simulations of macrodispersion in heterogeneous porous media," Water Resour. Res. **39**, 1135 (2002).

[13] G. Dagan, "Stochastic modeling of groundwater flow by unconditional and conditional probabilities. 2. The solute transport," Water Resour. Res. **18**, 835 (1982).

[14] L. W. Gelhar and C. L. Axness, "Three-dimensional stochastic analysis of macrodispersion in aquifers," Water Resour. Res. **19**, 161 (1983).

[15] J. Koplik, "Hydrodynamic dispersion in random networks," in *Disorder and Mixing*, edited by E. Guyon, J. P. Nadal, and Y. Pomeau (Kluwer Academic, Dordrecht, 1988), Chap. 7.

[16] C. Welty and L. W. Gelhar, "Stochastic analysis of the effects of fluid density and viscosity variability on macrodispersion in heterogeneous porous media," Water Resour. Res. **27**, 2061 (1991).

[17] C. T. Tan and G. M. Homsy, "Stability of miscible displacements in porous media: Rectilinear flow," Phys. Fluids **29**, 3549 (1986).

[18] G. I. Taylor, "Dispersion of soluble matter in solvent flowing slowly through a tube," Proc. R. Soc. London, Ser. A **219**, 186 (1953).

[19] N. Rakotomalala, D. Salin, and P. Watzky, "Miscible displacement between two parallel plates: BGK lattice gas simulations," J. Fluid Mech. **338**, 277 (1997).